Technical Note

Analysis and Evaluation of the Formation of a Heat Island in Tehran During Three Decades

Mohammad Javad Amiri *, Ali Sayyadi

Faculty of Environment, College of Engineering, University of Tehran, Tehran, Iran.

PAPER INFO	ABSTRACT
	The rising temperature of the earth's surface and the formation of heat islands in megacities have become two of the biggest environmental threats. This compound problem affects urban climatology, including urban vegetation and air pollution, human health, and the environment, including the group of vulnerable members of the society and public health, leading to the growing death rate. Hence, the purpose of this study is to investigate the leading causes of temperature changes and the development of a thermal island in the city of Tehran following the expansion of this metropolis in recent decades. This research uses thermal remote sensing and GIS techniques to analyze information from Landsat satellite images in (TM-ETM-TIRS) sensors from 1984 to 2020. The results of the research indicated that the surface temperature of the city of Tehran during the years 1984 to 1996, 1998 to 2008, and 2010 to 2020 experienced a relative increase in the summer and winter seasons. In the first decade, the average temperature of the green layer was -7, while the temperature of the magenta and red layers were 20 and 25 degrees, respectively. In the second decade, the average temperatures of the green and dark green classes were -1 and 3 while they were 23 and 27 degrees for the magenta and red classes, respectively. In the third decade, the average temperatures of the green and dark green classes were -1 and 3, and thost of the magenta and red layers increased to 28 and 31 degrees, respectively. Furthermore, the analysis of vegetation cover based on the NDVI index pointed to the continuing reduction of vegetation in the studied years. Regarding the direct correlation between the heat island and vegetation and the concentration of the heat island in the city center, further measures must be taken and the vegetation cover should be increased to reduce the heat island. The city center needs to be decentralized as part of the remedy via proper urban design and planning.

1. INTRODUCTION

Urban heat island is a situation that occurs in cities or metropolises primarily due to human-made changes on the earth's surface when urban areas experience higher temperatures than their rural areas (Mendez-Astudillo et al., 2021). Continuous extension of artificial surface including road constructions and building constructions as well as changes in radiation flux and climate have already intensified urban heat and formed urban hot spots (Tepanosyan et al., 2021). The expansion of artificial phenomena causes the creation of urban heat islands (El-Hadidy, 2021). Urban materials such as buildings, roads, and other asphalted areas are replaced by natural vegetation that leads to heat islands (Macintyre et al., 2021; Kabano et al., 2021). This temperature increase starts from 2 degrees and can be increased to several degrees (Harun et al., 2020).

The heat island causes irreversible damage to human life and our existing environment; the urban heat island is the most significant contributing factor affecting urban

climatology, including urban vegetation and air pollution (Li et al., 2022), including vulnerable groups, human health, and nature. It affects society (Wang et al., 2021) and public health (Sekertekin & Zadbagher, 2020; Vasenev et al., 2021) and increases death toll (Koopmans et al., 2021).

Land Surface Temperature (LST) is a key factor related to the earth's surface used at different scientific levels, such as weather forecast, hydrology, agriculture, public health, environmental science, etc. (Wei et al., 2021). It is also an important factor in global climate change, energy flux between the earth's surface and the atmosphere system, and the water cycle; therefore, its association with the environment has been widely studied (Ye et al., 2021; Gupta et al., 2019). LST is a key factor that controls physical, chemical, and biological processes at the interface between the earth and the atmosphere and greatly affects the state of vegetation and soil water (Chi et al., 2020).

Remote sensing is one of the main sources for estimating the amount of solar energy and preparing a map of LST in case of a lack of weather stations, specifically in land areas, oceans, and arid and semi-arid regions (Chi et al., 2020). The spatial resolution of sensors and the algorithms used to calculate solar

*Corresponding Author's Email: mjamiri@ut.ac.ir (M.J. Amiri)
URL: https://www.jree.ir/article_158621.html

radiation variables, vegetation indices, and land surface temperature are all factors measured using GIS remote sensing data (Al-Masaodi & Al-Zubaidi, 2021). Remote Sensing (RS) is a suitable method for directly acquiring experimental data and an effective means for environmental improvement, management, and monitoring urbanization dynamics. Geographical Information System (GIS) provides a spatial analysis, modeling, and mapping method. Many researchers have combined RS with GIS (Liu et al., 2021). Remote sensing satellites provide a simple way to investigate thermal differences between urban and rural areas, LST retrieval, and urban heat islands (Ahmed, 2017). The development of thermal remote sensing offers a good solution to the shortcomings observed in the conventional monitoring of urban heat islands. Such techniques can effectively quantify the distribution characteristics of urban heat islands and periodic and dynamic environmental changes (Wang et al., 2019). Today, a new generation of thermal remote sensing sensors such as MODIS (Medium Resolution Imaging Spectrometer), AVHRR (Very Advanced Resolution Radiometer), and ASTER (Medium Resolution Sensors) is used. Also, Landsat is practically free, and the oldest records in the archive have been used since the 1970s (Gadrani et al.,2018). The capital of Iran has experienced rapid urban development since the 1990s. Tehran is a key center for production, residence, trade, distribution, and transportation in Iran with a population of about 12 million people and is the first and most populous city in Iran (Mousavi-Baygi et al., 2010). The accelerated urban development of Tehran and lack of proper planning have important effects on its thermal environment. The political and geographical conditions of Tehran city and the damage of the heat island to humans and the environment have caused this research to investigate the process of the heat island using remote sensing.

1.1. Literature review

A review of the relevant literature and records shows that the term heat island was first proposed by Howard about a century ago, in 1833. Followed by further research, urbanization has caused significant changes in the meteorological parameters and features of the earth's surface and, as a result, has caused many changes in the local weather and climate. Mousavi et al. (2010); Akbari (2000); Weng (2009); Amiri et al (2009); Oke (1973) and Oke (1982) concluded in their studies that the island effect of heat was quite high on temperature than other meteorological quantities. They also stated that in a clear sky, weak wind and whirlwind presence could create suitable conditions for establishing a relatively intense heat island. In a study conducted in London between 1931 and 1960, the annual changes in air temperature were investigated. The average annual air temperature in this city, suburbs, and the surrounding rural areas was 11, 3, and 6 degrees Celsius, respectively, proving the existence of heat island in this city (Barry & Chorley, 1987). The first studies that attempted to investigate urban thermal landscapes using infrared thermal data used NOAA AVHRR sensor data. The areas in all these studies were 1.1 km, being suitable only for preparing a small map of the temperature on a city scale. Later, thermal infrared data of Landsat ETM, TM, and ASTER with spatial resolutions of 90, 60, and 120 meters, respectively, provided the possibility of extracting the surface temperature of the earth and a more accurate study of urban heat islands (Rizwan et al., 2008). Among the studies carried out in recent years,

those studies that use multi-temporal thermal images are more critical, because it is possible to discover the spatial-temporal changes of heat islands. A significant portion of the studies that have attempted to identify the spatio-temporal changes of heat islands used classical statistical methods (Rajeshwari & Mani, 2014). In another study conducted in Beijing, China, the values of the surface radiation temperature were extracted from a TM image of the Landsat satellite, and the creation of a heat island in this city was confirmed (Lam, 1990).

Recent studies for the city of Tehran show that minimum temperatures in Tehran have increased compared to the Varamin station, which indicates the release of much more thermal energy in Tehran than in its suburbs (Akbari, 2000). Studies related to Tehran's thermal island show that the effect of Tehran's thermal island has become more evident and along with the growth and development of the metropolis of Tehran, the spatial and temporal characteristics of the thermal island have changed. The spatial structure of the ground surface temperature, the effects of Tehran's thermal island, and the methods of obtaining temperature in hot and polluted areas are of particular importance (Sadeghinia et al., 2013). No study has evaluated the thermal trend components in the metropolis of Tehran so far, especially over period of 40 years. Yet, some research has been carried out without considering the influencing factors and the thermal island variations in the city and that these pieces of research suffered the limitation of short time period. To this end, considering the current challenges of the research including increase in the surface temperature of the city of Tehran and the emergence of a thermal island in this metropolis, it seems crucial to investigate the factors influencing the emergence of this problem. A spatial-spatial and biological environment view can be the way forward for this research. Therefore, in this research, the use of modern and practical technologies like remote sensing (thermal remote sensing), which has a general and spatial view of the city (the studied area of the city Tehran), and Geographic Information Systems (GIS), having the ability to perform various types of mapping and modeling and combining layers, the biological and environmental problems related to Tehran and the reasons for the emergence of a heat island in this city are investigated. For this purpose, this research aims to investigate the surface temperature of the city and its influencing factors and components in Tehran using remote sensing technology as well as Landsat satellite images and thermal bands from 1984 to 2020. Moreover, this study investigates and compares the trend of changes in the thermal component of Tehran over the last 40 years and three decades of study.

2. METHOD

2.1. The location of the study area

Tehran is the largest and most important city in Iran. The capital greatness and its particular political, economic, cultural, and geographical position and the concentration of information (compared to other parts of the country) have caused many people (for work, education, treatment, administrative affairs, buying or selling goods, and entertainment) to come to this city and settle gradually. With its current needs and development issues, this metropolis is run by about 24 government or public institutions. The municipality primarily organizes city issues and promotes citizen participation and satisfaction. The metropolis consists

of 22 districts. The location of Tehran, along with the divisions of the districts, can be seen in Figure 1.
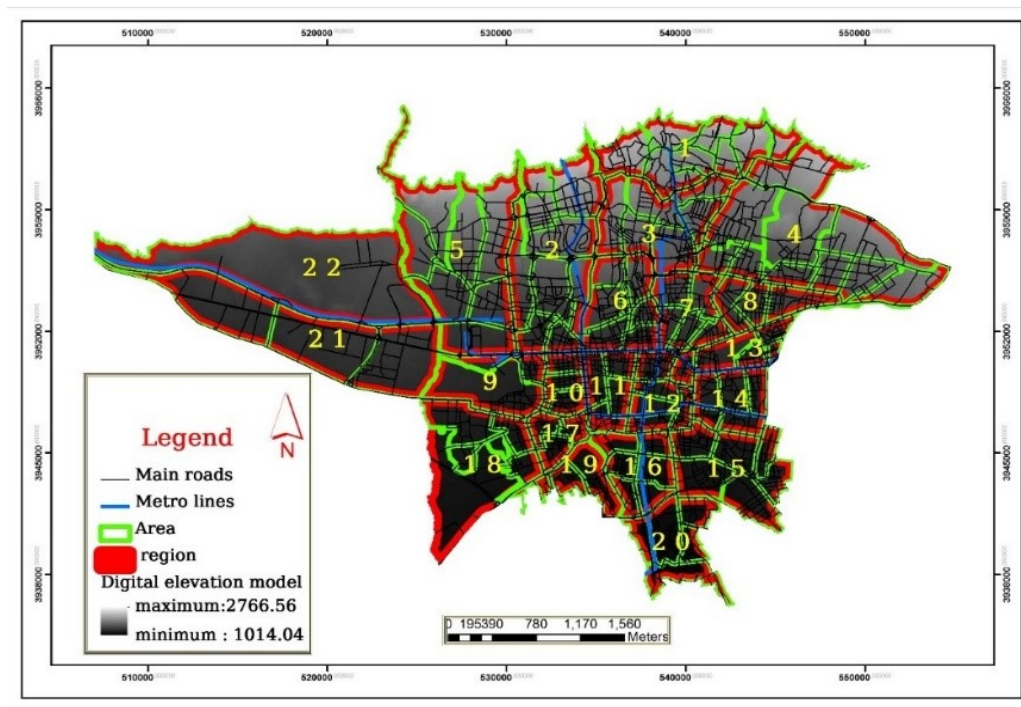
Figure 1. The geographical location of 22 districts of Tehran

2.2. Methodology

This is a descriptive-analytical and applied study in terms of purpose. In this study, Landsat satellite images are used for environmental and spatial analysis of Tehran. To this end, Landsat satellite images in TM, ETM+, and TIRS sensors from 1984 to 2020 are derived from the United States Geological Survey (USGS) and NASA website. This study aims to investigate (a) the changes in the climate and temperature of Tehran over the last 40 years and (b) the formation of a heat island in the city. One of the most important factors is the increase in LST which, as mentioned, is measured using thermal RS in summer and winter. Another factor is the study of vegetation in the area from 1984 to 2020 using the Normalized Difference Vegetation Index (NDVI) and Landsat Images.

Raw RS data collected from the land surface by various sensors are subject to shortcomings and errors. Therefore, deficiencies must be compensated and errors eliminated using satellite imagery.

ARC Gis 10.5 software is used here to generate output. IMAGIN ERDAS, Envi5.2, and IDRISI software are employed to process and analyze Landsat images and determine land use and thermal maps (Table 1). Table 1 shows the Landsat satellite imagery, sensors, and thermal bands used in this study. Landsat 5 and TM sensors were utilized from 1984 to 1998, Landsat 7 and ETM+ sensors were employed from 2000 to 2014, and Landsat 8 and OLI and TIRS sensors were applied from the year 2016 to 2020. Moreover, Band 6 and Bands 10 and 11 were utilized for ETM+ and TM sensors and TIRS sensors, respectively.

Table 1. Landsat satellite imagery specifications

Date of taking the image	Satellite	Sensor	PATH	ROW	Thermal band	Coordinate system
1984-04-25	LANDSAT_5"	"TM"	164	035	6	"WGS84"UTM_ZONE = 39
1984-11-19	LANDSAT_5"	"TM"	164	035	6	"WGS84"UTM_ZONE = 39
1987-07-07	LANDSAT_5"	"TM"	164	035	6	"WGS84"UTM_ZONE = 39
1987-01-12	LANDSAT_5"	"TM"	164	035	6	"WGS84"UTM_ZONE = 39
1990-07-31	LANDSAT_5"	"TM"	164	035	6	"WGS84"UTM_ZONE = 39
1990-12-22	LANDSAT_5"	"TM"	164	035	6	"WGS84"UTM_ZONE = 39
1992-01-26	LANDSAT_5"	"TM"	164	035	6	"WGS84"UTM_ZONE = 39
1992-08-05	LANDSAT_5"	"TM"	164	035	6	"WGS84"UTM_ZONE = 39
1994-01-15	LANDSAT_5"	"TM"	164	035	6	"WGS84"UTM_ZONE = 39
1994-08-27	LANDSAT_5"	"TM"	164	035	6	"WGS84"UTM_ZONE = 39
1996-08-23	LANDSAT_5"	"TM"	164	035	6	"WGS84"UTM_ZONE = 39

1996-10-10	LANDSAT_5"	"TM"	164	035	6	"WGS84"UTM_ZONE = 39
1998-01-26	LANDSAT_5"	"TM"	164	035	6	"WGS84"UTM_ZONE = 39
1998-08-06	LANDSAT_5"	"TM"	164	035	6	"WGS84"UTM_ZONE = 39
2000-01-16	"LANDSAT_7"	"ETM"	164	035	6	"WGS84"UTM_ZONE = 39
2000-08-11	"LANDSAT_7"	"ETM"	164	035	6	"WGS84"UTM_ZONE = 39
2002-01-13	"LANDSAT_7"	"ETM"	164	035	6	"WGS84"UTM_ZONE = 39
2002-08-09	"LANDSAT_7"	"ETM"	164	035	6	"WGS84"UTM_ZONE = 39
2004-01-19	"LANDSAT_7"	"ETM"	164	035	6	"WGS84"UTM_ZONE = 39
2004-08-14	"LANDSAT_7"	"ETM"	164	035	6	"WGS84"UTM_ZONE = 39
2006-02-25	"LANDSAT_7"	"ETM"	164	035	6	"WGS84"UTM_ZONE = 39
2006-08-04	"LANDSAT_7"	"ETM"	164	035	6	"WGS84"UTM_ZONE = 39
2008-01-14	"LANDSAT_7"	"ETM"	164	035	6	"WGS84"UTM_ZONE = 39
2008-08-09	"LANDSAT_7"	"ETM"	164	035	6	"WGS84"UTM_ZONE = 39
2010-01-03	"LANDSAT_7"	"ETM"	164	035	6	"WGS84"UTM_ZONE = 39
2010-08-15	"LANDSAT_7"	"ETM"	164	035	6	"WGS84"UTM_ZONE = 39
2012-01-25	"LANDSAT_7"	"ETM"	164	035	6	"WGS84"UTM_ZONE = 39
2012-08-04	"LANDSAT_7"	"ETM"	164	035	6	"WGS84"UTM_ZONE = 39
2014-01-14	"LANDSAT_7"	"ETM"	164	035	6	"WGS84"UTM_ZONE = 39
2014-08-10	"LANDSAT_7"	"ETM"	164	035	6	"WGS84"UTM_ZONE = 39
2016-02-03	"LANDSAT_8"	"OLI_TIRS"	164	035	11-10	"WGS84"UTM_ZONE = 39
2016-08-15	"LANDSAT_8"	"OLI_TIRS"	164	035	11-10	"WGS84"UTM_ZONE = 39
2018-01-25	"LANDSAT_8"	"OLI_TIRS"	164	035	11-10	"WGS84"UTM_ZONE = 39
2018-08-05	"LANDSAT_8"	"OLI_TIRS"	164	035	11-10	"WGS84"UTM_ZONE = 39
2020-01-15	"LANDSAT_8"	"OLI_TIRS"	164	035	11-10	"WGS84"UTM_ZONE = 39
2020-08-10	"LANDSAT_8"	"OLI_TIRS"	164	035	11-10	"WGS84"UTM_ZONE = 39

2.3. Parameters affecting LST

2.3.1. Land use

One factor affecting the temperature increase in Tehran is changes in land use. Examples include changes in land use, excessive space use, building densities, and urban areas. Changes in the type of land use and society's tendency to intervene in space reflect the structure of the space economy in cities. The space economy in Tehran is based on developing high-price and high-quality urban lands in the affluent areas of the city. The predominant trends included residential, commercial, office, and tourism spaces. The most significant demand involves changing the use of green space, residential spaces, and development reserve lands.

Studies show that the space economy in Tehran is based on the development of high-price and high-quality urban lands in the affluent areas of this city. The high concentration of these interventions can be seen at Districts 1, 2, and 3. Trends in land-use interventions and changes in Tehran are not balanced. The spatial distribution pattern of land use and spatial autocorrelation indicate that the predominant trend involves residential, commercial, office, and tourism uses and that a tremendous demand for land-use change is changing the use of green space residential spaces and development reserve

lands. Continuation of this process has caused excessive use of building surfaces instead of vegetation and garden and, consequently, an increase in temperature at the districts of Tehran. Remote sensing, which aims to identify and separate land phenomena and classify them, and Landsat satellite imagery from 1984 to 2020 are used to study these changes. Band composition in Landsat images is one of the methods used to obtain a land-use map before classification. In this study, the 2-3-4 band combination is used for TM and ETM+ while the 2-3-5 band composition is applied to the TIRS sensor. In this combination, Band 4 is the infrared band, with the vegetation having the highest reflectance. Band compositions for preparing land-use maps for Tehran from 1984 to 2020 can be seen in Figures 2 and 3. As seen in the figure, the study area is divided into five classes (green space and vegetation in green, urban land use in pink, barren and abandoned lands in white, poor lands or mountains in purple, and roads in black). Land-use changes for studying the heat island in Tehran are quite evident with further expansion of the thermal island due to reduced vegetation and increased urban land use. According to Figure 2, from 1984 to 2004, Tehran was divided into 2 parts, the urban part at the center and the outside where barren and inferior lands covered with vegetation lie. Over time, poor quality of land and life along

with useless vegetation have transformed into the city (residential areas and roads). Based on Figure 3, from 2006 to 2020, the green part (vegetation) changed to pink (city) and the vegetation was reduced a lot in 2018 and 2020, being one of the factors in increasing the temperature of the earth's surface.
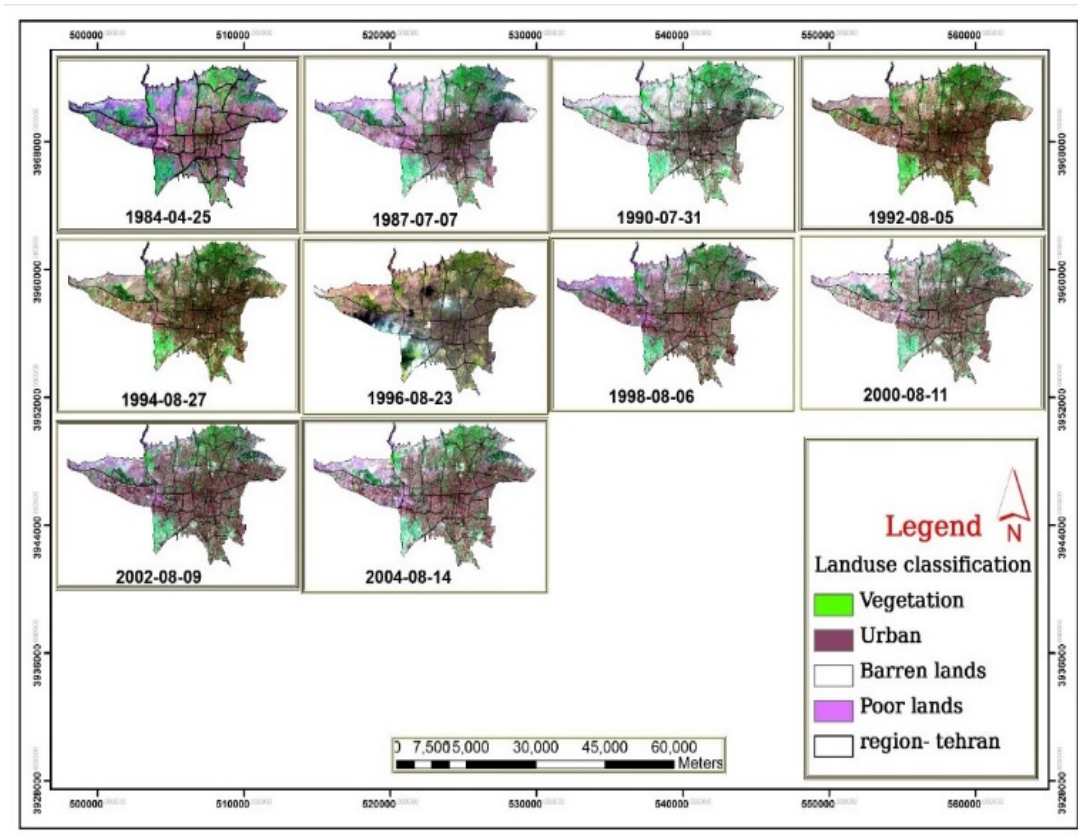

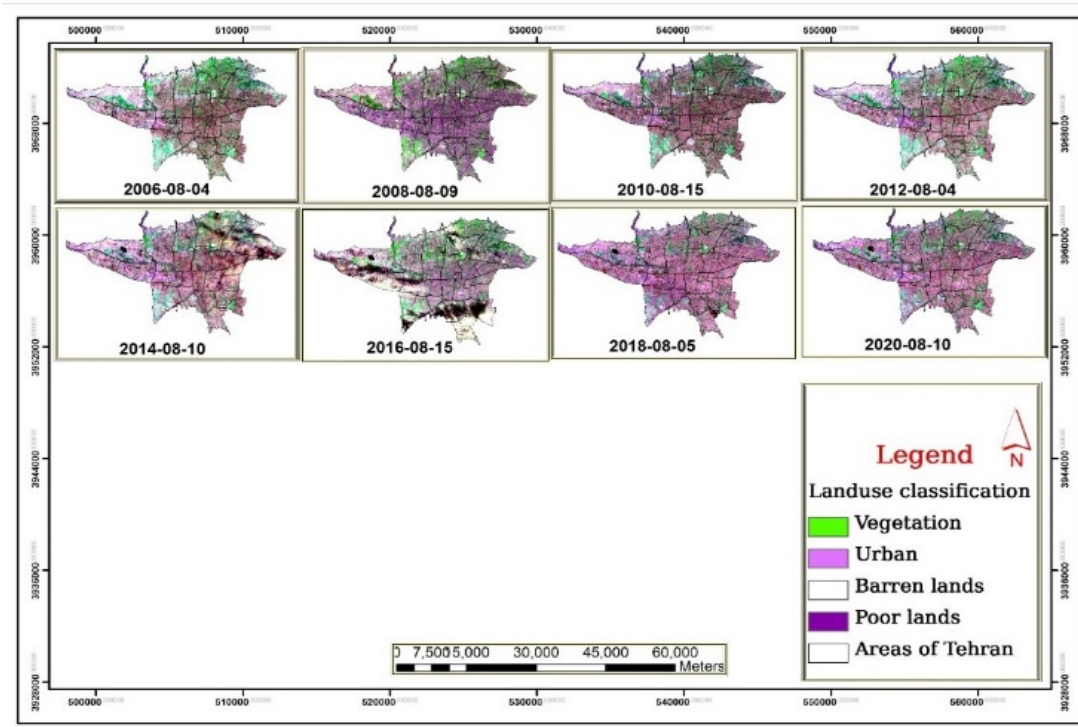**Figure 2.** Land-use map of Tehran from 1984 to 2004

Figure 3. Land-use map of Tehran from 2006 to 2020

2.3.2. Land Surface Temperature (LST)

One of the most critical factors affecting the increase in temperature of Tehran is LST, which is obtained using the thermal bands of Landsat satellite in TM, ETM+, and TIRS sensors. The pixels of the images must first be processed to obtain correct information to prepare a thermal map of the

city. All of these are called image pre-processing or image correction. One of the most critical corrections made to image pixels is radiometric. One part of radiometric corrections of the images is spectral correction performed on digital numbers (DN) or the pixel such that when the image is taken, it has DN. These DNs contain information about land surface phenomena. However, the initial data contain basic information (uncorrected) and cannot represent the parameters of the land surface, such as temperature, humidity, vegetation, etc. The DN of the satellite imagery must be corrected to apply the values of the ground surface parameters to the desired satellite imagery. The DN of each image must be converted into radiance and reflectance. This form of correction is referred to as spectral correction. Several models and methods for converting DN of satellite images into radiance and reflectance are given in the following. Equation (1) (Chander et al., 2009) converts raw image values into radiance for Landsat TM and ETM images.

$$L\lambda = (\frac{LMAX-LMIN}{Qcalmax-Qcalmin})\,(Qcal - Qcalmin) + LMIN \qquad (1)$$

where $L\lambda$ is the spectral radiance in the sensor, Qcal is the pixel value (DN) in the desired band, Qcalmin is the minimum pixel value (DN), Qcalmax is the maximum pixel value (DN), and LMIN and LMAX are minimum and maximum spectral radiances, respectively, in the sensor.

$$p\lambda = \frac{\pi \times L\lambda \times d^2}{ESUN\,\lambda \times COS\,\theta S} \qquad (2)\,(Chander\ et\ al.,\ 2009)$$

where $p\lambda$ is the reflectance coefficient, $\pi = 3.1459$, $L\lambda$ is the spectral radiance in the sensor, d is the distance between the earth and the sun (astronomical unit), ESUN is the average of the sun's rays, and θ is the angle of the sun's rays (degrees).

Equation (3) (Chander et al., 2009) is employed to obtain the spectral radiance in the OLI sensor:

$$L\lambda = ML * Qcal + AL \qquad (3)$$

where $L\lambda$ is the radiance above the atmosphere (watts/m^2*srad*μm), ML is the multiplicative conversion factor, Qcal includes the pixel values (DNs) of 10 and 11, and AL is the aggregate conversion factor.

2.3.3. Obtaining the brightness temperature

Thermal band data can be converted from spectral radiance in the sensor into brightness temperature, assuming that the earth is a black body and includes the effects of the atmosphere (absorption and radiance). The brightness temperature for Landsat satellite sensors is calculated using Equation (4) (Rajeshwari & Mani, 2014).

$$T = \frac{K2}{Ln(\frac{K1}{L\lambda}+1)} \qquad (4)$$

where T is the temperature affecting the brightness in the sensor in Kelvin, K2 is the calibration coefficient 2 in Kelvin, K1 is the calibration coefficient 1 in W (m st μm), and $L\lambda$ is the spectral radiance in the sensor. The coefficients K1 and K2 are calculated according to Table 2.

Satellite images of Tehran are calibrated and the necessary corrections are made. The mentioned algorithms are used to prepare thermal maps and the thermal zoning map of Tehran is compiled covering the years 1984 to 2020.

Table 2. Coefficients K1 and K2 for Landsat satellite

Sensor coefficient (band)	Calibration coefficient 1	Calibration coefficient 2 (in K)
L5-TM B6	607.76	1260.56
L7-ETM+B6	666.09	1282.71
L8-OLI B10	777.89	1321.08
L8-OLI B11	480.89	1201.14

2.3.4. Vegetation

One of the other factors affecting the temperature increase in Tehran is its vegetation density, which is obtained using Landsat satellite images and NDVI.

One of the most well-known, simplest, and most widely used indices in vegetation studies is NDVI. It has a simple computational process and has higher dynamic power than other indices. This index has the highest sensitivity to vegetation changes and is less sensitive to the effects of weather and soil, except in cases where vegetation is low. NDVI is calculated using Equation (5) (Van de Griend & Owe, 1993):

$$NDVI = \frac{NIR-RED}{NIR+RED} \qquad (5)$$

where NIR and RED are the reflectance and reflectance at the infrared and red bands, respectively. Although theoretically, the value of this index is in the range of -1 to 1, in practice, it is less than 1 and more than -1. The values of this index for dense vegetation tend to be 1, but negative values characterize clouds, snow, and water. In addition, the rocks and barren soils with similar spectral reactions used at the two bands are seen with values close to zero. Based on this index, typical soil is considered equal to 1. The higher the pixel distance from the soil size, the denser the vegetation. In this regard, NDVI is applied to Landsat images, and the vegetation map of Tehran is prepared from 1984 to 2020 in five classes: very light red, relatively light orange, medium-density yellow, relatively high light green, and very high-density dark green.

3. RESULTS AND DISCUSSION

One of the most critical factors affecting the increase in temperature in Tehran is LST. This study prepared a thermal zoning map based on Landsat thermal images in ETM and TM sensors at Band 6 and TIRS sensors at Bands 10 and 11 in winter and summer from 1984 to 2020. The thermal zoning map of Tehran was divided from minimum to maximum temperature into eight classes, including green, dark green, blue, light blue, yellow, orange, pink, and red in three time periods 1984 to 1996, 1998 to 2008, and 2010 to 2020, each of which is explained separately.

3.1. Thermal zoning map of Tehran from 1984 to 1996

The thermal zoning map of Tehran from 1984 to 1996 can be seen in Figure 4. According to the figure, the largest zones belong to the yellow, coral, and magenta classes, while the lowest zones belong to the green, sea green, and cyan classes.

LST is divided into eight classes in Table 3. According to the table, the minimum temperature of -5 °C belongs to the

year 1984, while the maximum temperature of 51 °C belongs to the year 1987. Figure 5 shows the average LST of -7 °C for the green class from 1984 to 1996 and the average LST of 20 and 25 °C for the magenta and red classes, respectively.
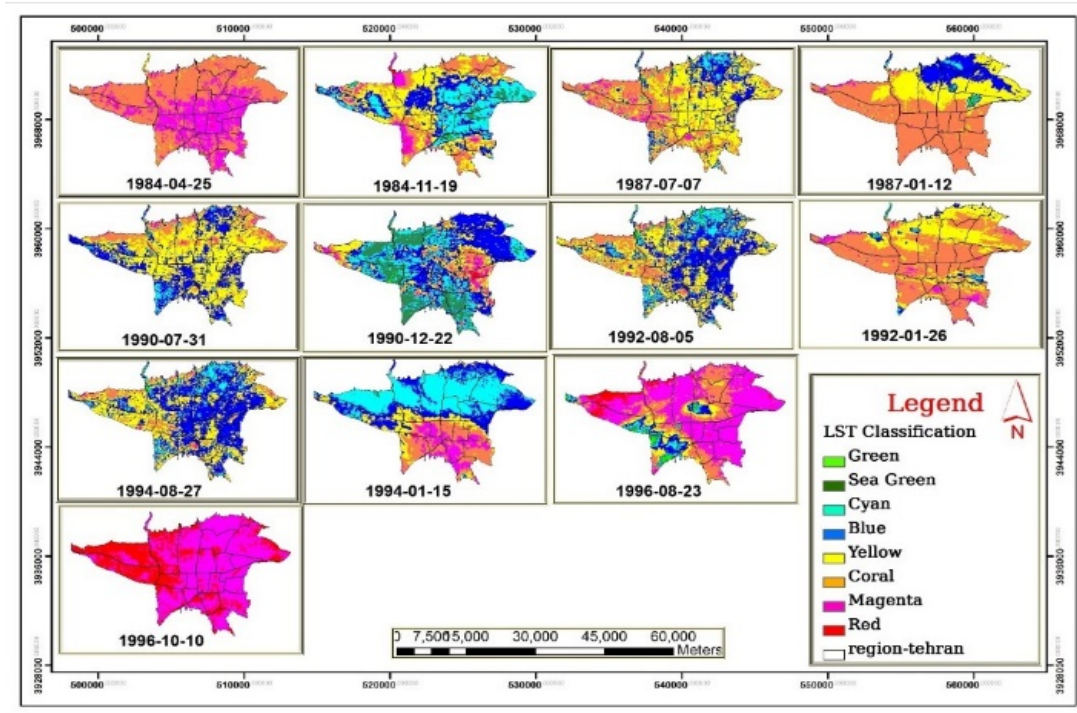

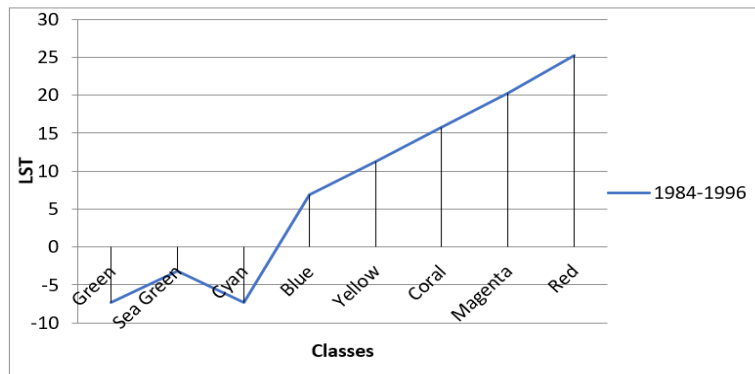**Figure 4.** LST map of Tehran from 1984 to 1996

Figure 5. Average LST in Tehran from 1984 to 1996

Table 3. LST in Tehran from 1984 to 1996

Year	Class temperature (°C)							
	Green	**Sea Green**	**Cyan**	**Blue**	**Yellow**	**Coral**	**Magenta**	**Red**
1984-04-25	-05 - -0	-0 - 04	04 - 09	09 - 14	14 - 19	19 - 24	24 - 29	29 - 34
1984-11-19	-27 - -25	-25 - -22	-22 - -20	-20 - -18	-18 - -15	-15 - -13	-13 - -11	-11 - -08
1987-07-07	23 - 26	26 - 30	30 - 33	33 - 37	37 - 40	40 - 44	44 - 47	47 - 51
1987-01-12	-18 - -23	-18 - -13	-13 - -08	-08 - -02	-02 - 02	02 - 07	07 - 12	12 - 18
1990-07-31	19 - 23	23 - 26	26 - 30	30 - 33	33 - 37	37 - 41	41 - 44	44 - 48
1990-12-22	-20 - -17	-17 - -14	-14 - -11	-11 - -08	-08 - -05	-05 - -03	-03 - -0	-0 - 02
1992-01-26	-26 - -21	-21 - -17	-17 - -13	-13 - -09	-09 - -04	-04 - -0	-0 - -03	03 - 07
1992-08-05	22 - 25	25 - 27	27 - 30	30 - 32	32 - 35	35 - 37	37 - 40	40 - 43
1994-01-15	-15 - -12	-12 - -08	-08 - -05	-05 - -02	-02 - 0	0 - 03	03 - 07	07 - 10
1994-08-27	23 - 26	26 - 29	29 - 32	32 - 34	34 - 37	37 - 40	40 - 43	43 - 46
1996-08-23	-14 - -06	-06 - 01	01 - 08	08 - 16	16 - 24	24 - 32	32 - 39	39 - 47
1996-10-10	-71 - -57	-57 - -44	-44 - -30	-30 - -16	-16 - -03	-03 - 10	10 - 24	24 - 37

The trend of LST classes from 1984 to 1996 can be seen in Figure 6.

Figure 7 shows changes in LST classes from 1984 to 1996.

3.2. Thermal zoning map from 1998 to 2008

The thermal zoning map of Tehran from 1998 to 2008 can be seen in Figure 8. As can be seen, the highest thermal zones belong to the yellow, coral, and magenta classes.

LST classes (8 classes) can be seen in Table 4. According to the table, the average LST of green and sea green classes included -1 and 3 °C respectively, and the average LSTs of magenta and red classes were 23 and 27 °C, respectively, from 1984 to 1996. Figure 9 shows average LST in Tehran from 1998 to 2008. Changes in LST classes from 1998 to 2008 can be seen in Figure 10.

Figure 11 shows the changes in LST classes in Tehran from 1998 to 2008.
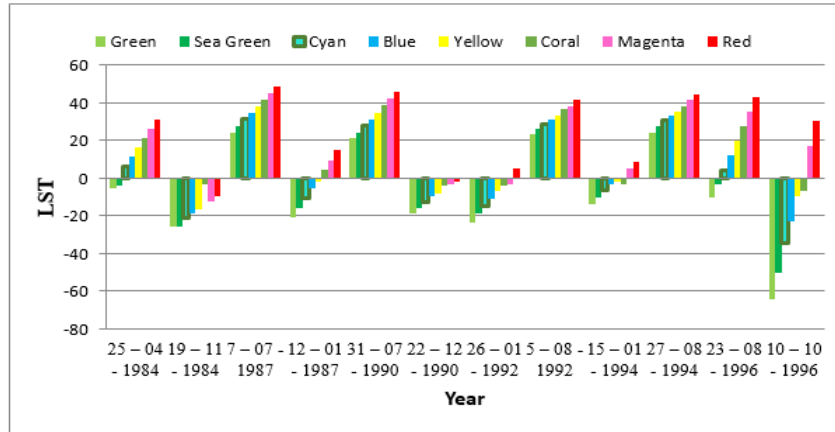
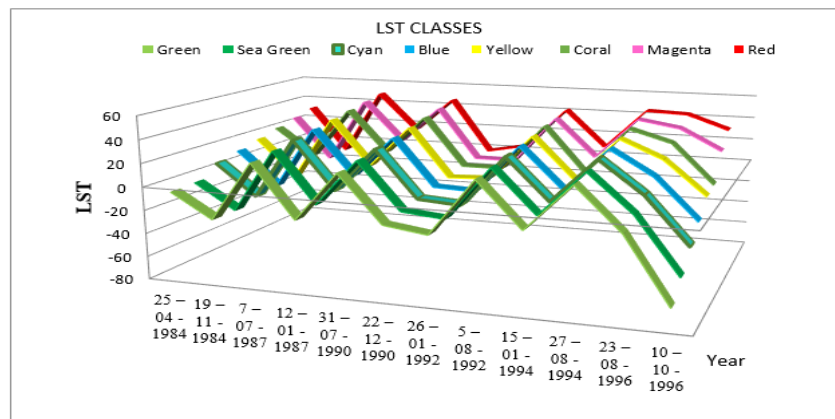**Figure 6.** LST classes in Tehran from 1984 to 1996

Figure 7. The trend of changes in LST classes in Tehran from 1984 to 1996
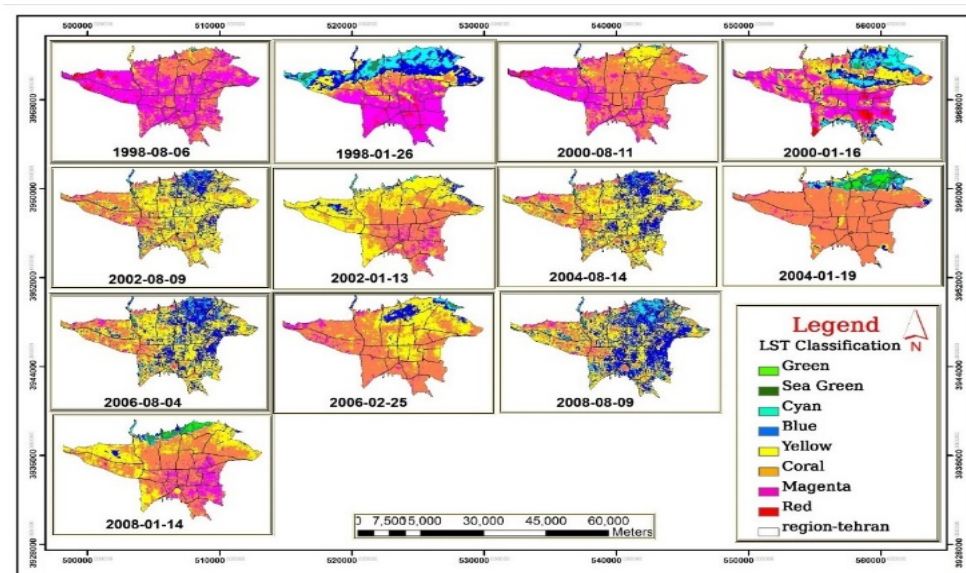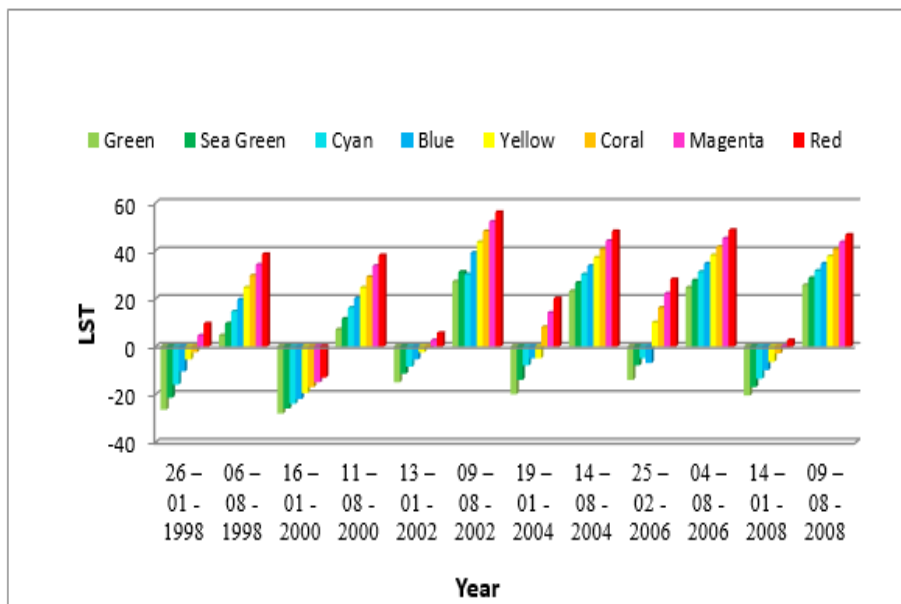

Figure 8. LST map of Tehran from 1998 to 2008

Table 4. LST in Tehran from 1998 to 2008

Year	Classes							
	Green	**Sea Green**	**Cyan**	**Blue**	**Yellow**	**Coral**	**Magenta**	**Red**
1998-01-26	-29 - -24	-24 - -19	-19 - -13	-13 - -08	-08 - -03	-03 - 02	02 - 07	07 - 12
1998-08-06	02 - 07	07 - 12	12 - 17	17 - 22	22 - 27	27 - 32	32 - 36	36 - 41
2000-01-16	-29 - -27	-27 - -25	-25 - -23	-23 - -21	-21 - -18	-18 - -16	-16 - -14	-14 - -12
2000-08-11	05 - 09	09 - 14	14 - 18	18 - 22	22 - 27	27 - 31	31 - 36	36 - 40
2002-01-13	-17 - -13	-13 - -10	-10 - -07	-07 - -04	-04 - -01	-01 - 01	01 - 04	04 - 07
2002-08-09	25 - 29	29 - 33	33 - 37	37 - 41	41 - 46	46 - 50	50 - 54	54 - 58
2004-01-19	-23 - -17	-17 - -11	-11 - -05	-05 - -0	-0 - 05	05 - 11	11 - 17	17 - 23
2004-08-14	21 - 25	25 - 28	28 - 32	32 - 35	35 - 39	39 - 42	42 - 46	46 - 50
2006-02-25	-17 - -11	-11 - -05	-05 - 0	0 - 07	07 - 13	13 - 19	19 - 25	25 - 31
2006-08-04	23 - 26	26 - 29	29 - 33	33 - 36	36 - 40	40 - 43	43 - 47	47 - 50
2008-01-14	-22 - -19	-19 - -15	-15 - -12	-12 - -08	-08 - -05	-05 - -01	-01 - 01	01 - 04
2008-08-09	24 - 27	27 - 30	30 - 33	33 - 36	36 - 39	39 - 42	42 - 45	45 - 48

Figure 9. Average LST in Tehran from 1998 to 2008

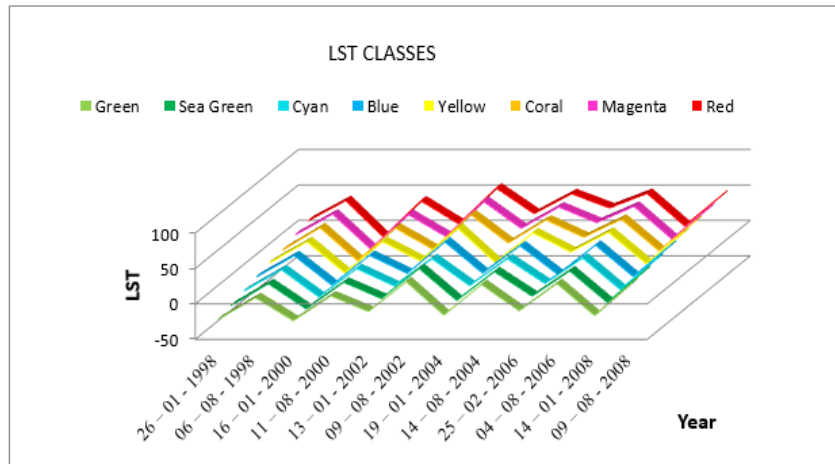**Figure 10.** Changes in LST classes in Tehran from 1998 to 2008

Figure 11. The trend of changes in LST classes in Tehran from 1998 to 2008

3.3. Thermal zoning map of Tehran from 2010 to 2020

Figure 12 shows the thermal zoning map of Tehran from 2010 to 2020. As can be seen, the highest thermal zones belong to the yellow, blue, and magenta classes.

Table 5 shows the LST classes (eight classes). The average LST of -1 and 3 °C for the green and sea green classes, respectively, and the average LST of 28 and 31 °C for the magenta and red classes, respectively, from 2010 to 2020 can be seen in Figure 13.
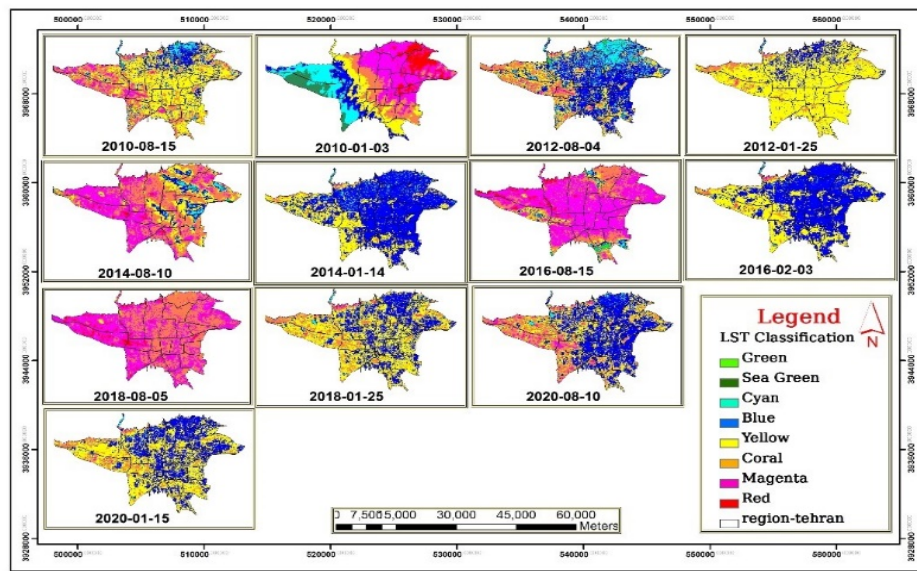

Figure 12. LST map of Tehran from 2010 to 2020

Table 5. LST in Tehran from 2010 to 2020

| Year	Classes							
	Green	**Sea green**	**Cyan**	**Blue**	**Yellow**	**Coral**	**Magenta**	**Red**
2010-01-03	-48 - -42	-42 - -35	-35 - -29	-29 - -22	-22 - -16	-16 - -09	-09 - -03	-03 - 03
2010-08-15	19 - 22	22 - 25	25 - 29	29 - 32	32 - 35	35 - 38	38 - 41	41 - 44
2012-01-25	-17 - -12	-12 - -07	-07 - -02	-02 - 02	02 - 07	07 - 12	12 - 17	17 - 22
2012-08-04	22 - 25	25 - 28	28 - 31	31 - 34	34 - 37	37 - 40	40 - 43	43 - 46
2014-01-14	-09 - -05	-05 - -01	-01 - 03	03 - 07	07 - 11	11 - 15	15 - 20	20 - 24
2014-08-10	-02 - 04	04 - 11	11 - 18	18 - 25	25 - 32	32 - 39	39 - 46	46 - 53
2016-02-03	26 - 27	27 - 27	27 - 28	28 - 28	28 - 29	29 - 29	29 - 30	30 - 31
2016-08-15	-12 - -05	-05 - 02	02 - 09	09 - 17	17 - 24	24 - 32	32 - 39	39 - 47
2018-01-25	-05 - -01	-01 - 02	02 - 06	06 - 10	10 - 14	14 - 18	18 - 22	22 - 26
2018-08-05	-05 - 01	01 - 08	08 - 15	15 - 22	22 - 30	30 - 37	37 - 44	44 - 51
2020-01-15	-14 - -10	-10 - -06	-06 - -01	-01 - 02	02 - 06	06 - 11	11 - 15	15 - 20
2020-08-10	16 - 20	20 - 24	24 - 28	28 - 33	33 - 37	37 - 41	41 - 45	45 - 49
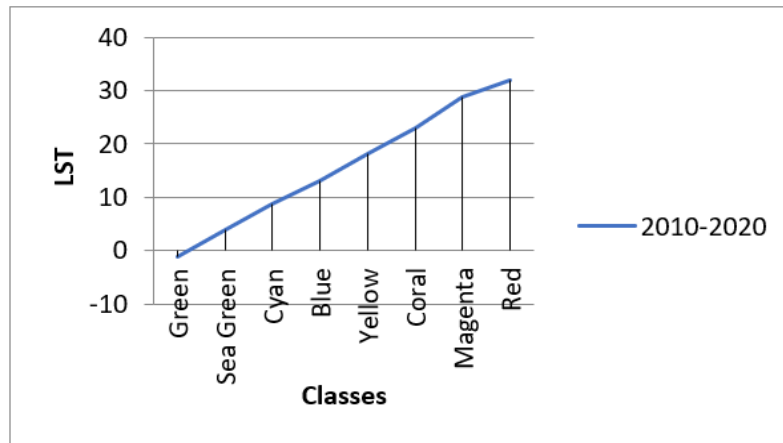
Figure 13. Average LST in Tehran from 2010 to 2020

Figure 14 shows the changes in LST classes in Tehran from 2010 to 2020.

The trend of changes in LST classes in Tehran from 2010 to 2020 can be seen in Figure 15.

According to the thermal zoning map, figures, and tables, the temperature in Tehran over the last 40 years and within the interval of three periods from 1984 to 1996, 1998 to 2008, and 2010 to 2020 in winter and summer has increased significantly. If this trend continues, there will be no winters or cold seasons in Tehran in the future and hot weather will replace colder weather. NDVI was also used to study the vegetation trend in Tehran. The index was prepared for Landsat images from 1984 to 2020. It was classified into four classes: Very low density in red, relatively low density in coral, medium density in green, and very high density in sea green. The results of the NDVI maps show the declining trend of vegetation over the last 40 years (Figures 16 and 17).
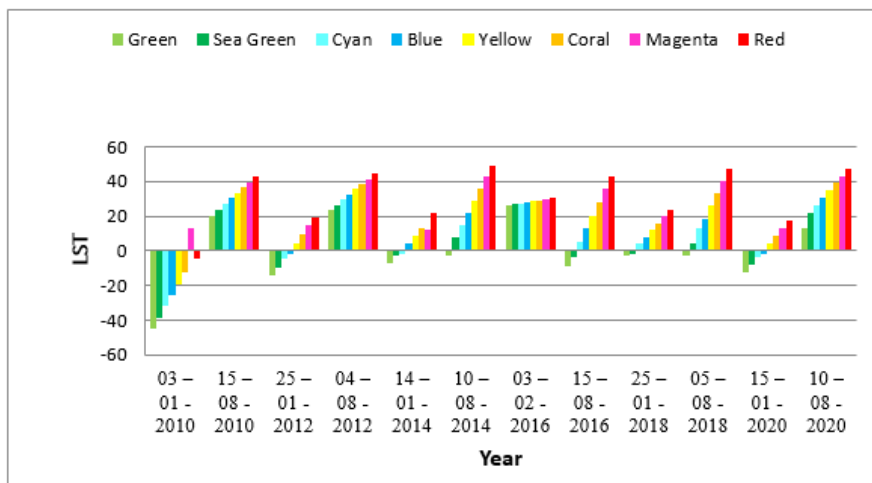

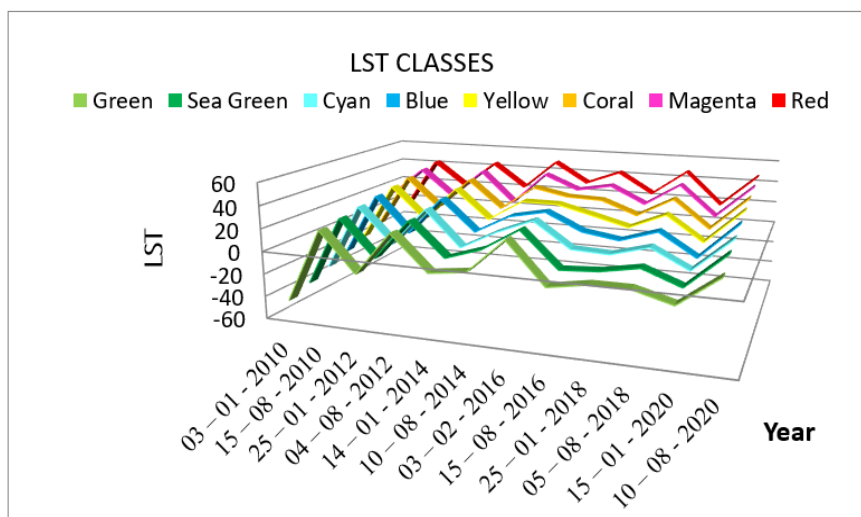**Figure 14.** LST classes in Tehran from 2010 to 2020

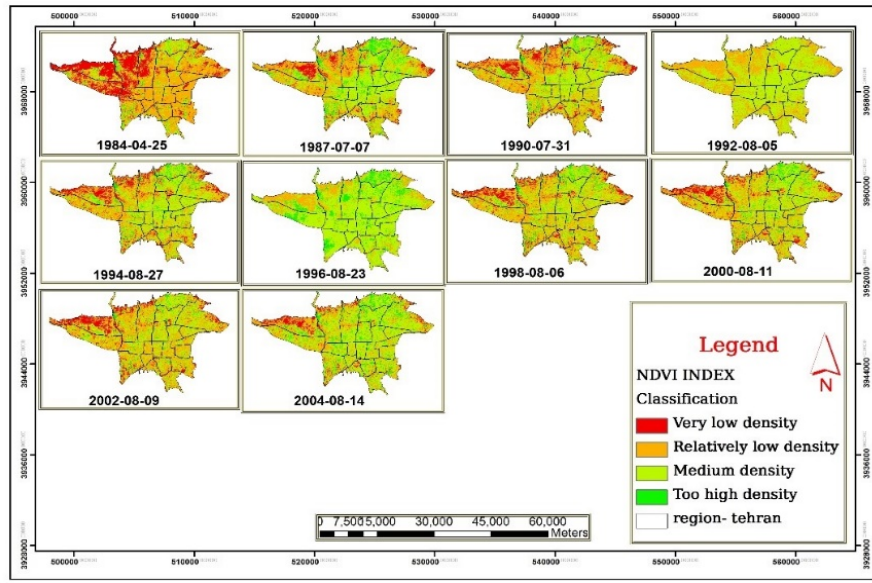**Figure 15.** The trend of changes in LST classes from 2010 to 2020

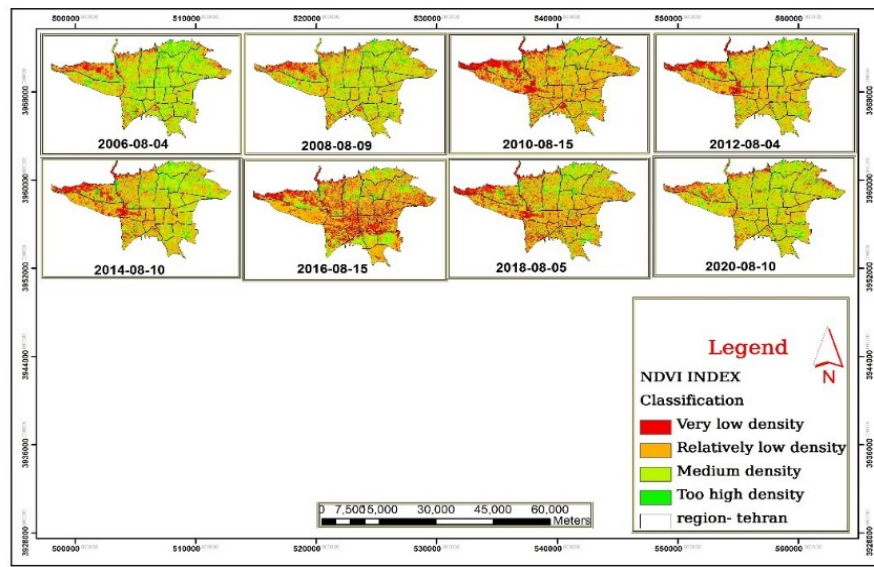**Figure 16.** NDVI map of Tehran from 1984 to 2004

Figure 17. NDVI map of Tehran from 2008 to 2020

4. CONCLUSIONS

The increase in temperature and heat islands directly impacts urban vegetation and air, human health, and the environment and causes increased mortality. In the process of controlling and monitoring the heat island, one should keep in mind that the thermal change and increase depend on many factors. Mousavi et al (2010); Akbari (2000); Weng (2009) and Amiri et al (2009) realized that these many factors were uncontrollable climatic ones including solar radiation, wind intensity, etc. However, other factors are controllable and include human activities in the environment, changing the state of the earth's natural surface, and replacing vegetation with urban materials such as buildings, roads, and other asphalt areas, which can cause an increase in temperature. According to the stated problems and the possibility of controlling the second category of factors, the main goal of this research is to investigate the temperature changes in the city and the components and factors influencing its formation. Considering that no research has implemented the unique evaluation process of the thermal component of Tehran

metropolis over the last 40 years, or perhaps there are some studies that faied to consider the influencing factors, a survey of the land surface temperature, vegetation, and temperature in Tehran seems to be necessary.

The Use-Land survey demonstrated that Tehran was divided into two parts: the urban part located at the center and the outside covering barren lands, lowlands, and vegetation. Nevertheless, in recent decades, the barren lands and vegetation have been urbanized and transformed (residential areas and roads). The survey (LST) illustrated that the minimum and maximum temperatures were -5 °C and 51 °C in 1984 and 1987, respectively. The LST recorded in each decade has changed from 20 and 25 to 23 and 27. In the last decade, LST has changed from 23 and 27 to 28 and 31 degrees. NDVI survey showed that NDVI had had a decreasing trend in the last 40 years. The review of Tehran temperature over the years indicates that Tehran's temperature increases significantly in the winter and summer. If this trend continues, there will be no winter and cold season in Tehran in the future. Based on the results and evident factors, the rising

trend of temperature in Tehran continues and will cause irreparable damage.

Heat islands can be controlled by proper city designing and vegetation management (increasing green roofs, parks, etc.), and heat flow at the center of the city should be managed, which requires urban planning and use of remote sensing in design and use. In the end, it is recommend that future research be examined regionally according to the size of the city. Besides, the impact of the relationship between the types of structures and roads on the increase of heat islands be examined.

5. ACKNOWLEDGEMENT

REFERENCES

1. Ahmed, S. (2017). Assessment of urban heat islands and impact of climate change on socioeconomic over Suez Governorate using remote sensing and GIS techniques. *The Egyptian Journal of Remote Sensing and Space Sciences, 21*(1), 15-25. https://doi.org/10.1016/j.ejrs.2017.08.001

2. Akbari, H. (2000). Consideration of temperature distribution pattern of Tehran using Landsat TM thermal data [MA dissertation, Tarbiat Modarres University]. https://ganj.irandoc.ac.ir (In Persian).

3. Al-Masaodi, H.J.O., & Al-Zubaidi, H.A.M. (2021). Spatial-temporal changes of land surface temperature and land cover over Babylon Governorate, Iraq. *Materials Today: Proceedings*. https://doi.org/10.1016/j.matpr.2021.05.179

4. Amiri, R., Weng, Q., Alimohammadi, A., & Alavipanah, S.K. (2009). Spatial-temporal dynamics of land surface temperature in relation to fractional vegetation cover and land use/cover in the Tabriz urban area, Iran. *Remote Sensing of Environment, 113* (12, 15), 2606-2617. https://doi.org/10.1016/j.rse.2009.07.021

5. Barry, R., & Chorley, R.J. (1987). Atmosphere, weather and climate. London: Methuen and co. Ltd. https://www.routledge.com/Atmosphere-Weather-and-Climate/Barry-Chorley/p/book/9780415465700

6. Chander, G., Markham, B., & Helder, D. (2009). Summary of current radiometric calibration coefficients for Landsat MSS, TM, ETM+, and EO-1 ALI sensors". *Remote Sensing of Environment, 113*(5), 893-903. https://doi.org/10.1016/j.rse.2009.01.007

7. Chi, Y., Sun, J., Sun, Y., Liu, Sh., & Fu, Zh. (2020). Multi-temporal characterization of land surface temperature and its relationships with normalized difference vegetation index and soil moisture content in the Yellow River Delta, China. *Global Ecology and Conservation, 23*, Article Number: (e01092). https://doi.org/10.1016/j.gecco.2020.e01092

8. El-Hadidy, Sh.M. (2021). The relationship between urban heat islands and geological hazards in Mokattam plateau, Cairo, Egypt. *The Egyptian Journal of Remote Sensing and Space Sciences, 24*(3, Part 2), 547-557. https://doi.org/10.1016/j.ejrs.2021.02.004

9. Gadrani, L., Lominadze, G., & Tsitsagi, M. (2018). F Assessment of landuse/landcover (LULC) change of Tbilisi and surrounding area using remote sensing (RS) and GIS. *Annals of Agrarian Science , 16* (2), 163-169. https://doi.org/10.1016/j.aasci.2018.02.005

10. Gupta, N., Mathew, A., & Khandelwal, S. (2019). Analysis of cooling effect of water bodies on land surface temperature in the nearby region: A case study of Ahmedabad and Chandigarh cities in India. *The Egyptian Journal of Remote Sensing and Space Sciences, 22*(1), 81-93. https://doi.org/10.1016/j.ejrs.2018.03.007

11. Harun, Z., Reda, E., Abdulrazzaq, A., Amer Abbas, A., Yusup, Y., & Zaki, Sh.A. (2020). Urban heat island in the modern tropical Kuala Lumpur: Comparative weight of the different parameters. *Alexandria Engineering Journal, 59*(6), 4475-4489. https://doi.org/10.1016/j.aej.2020.07.053

12. Kabano, P., Lindley, S., & Harris, A. (2021). Evidence of urban heat island impacts on the vegetation growing season length in a tropical city. *Landscape and Urban Planning, 206*, Article Number: 103989. https://doi.org/10.1016/j.landurbplan.2020.103989

13. Koopmans, S., Heusinkveld, B.G., & Steeneveld, G.J. (2020). A standardized physical equivalent temperature urban heat map at 1-m spatial resolution to facilitate climate stress tests in the Netherlands. *Building and Environment, 181*(15), Article Number: (106984). https://doi.org/10.1016/j.buildenv.2020.106984

14. Lam, N.S.N. (1990). Description and measurement of Landsat TM images using fractals. *Photogrammetric Engineering and Remote Sensing, 56*, 187-195. https://www.asprs.org/wp-content/uploads/pers/1990journal/feb/1990_feb_187-195.pdf

15. Li, H., Zhou, Y., Jia, G., Zhao, K., & Dong, J. (2022). Quantifying the response of surface urban heat island to urbanization using the annual temperature cycle model. *Geoscience Frontiers , 13*(1). Article Number: 101141. https://doi.org/10.1016/j.gsf.2021.101141

16. Liu, Ch., Yang, M., Hou, Y., Zhao, Y., & Xue, X. (2021). Spatiotemporal evolution of island ecological quality under different urban densities: A comparative analysis of Xiamen and Kinmen Islands, Southeast China. *Ecological Indicators, 124*, Article Number: 107438. https://doi.org/10.1016/j.ecolind.2021.107438

17. Macintyre, H.L., Heaviside, C., Cai, X., & Phalkey, R. (2021). The winter urban heat island: Impacts on cold-related mortality in a highly urbanized European region for present and future climate. *Environment International, 154*, Article Number: 106606. https://doi.org/10.1016/j.envint.2021.106530

18. Mendez-Astudillo, J., Lau, L., Tang, Y.T., & Moore, T. (2021). A new Global Navigation Satellite System (GNSS) based method for urban heat island intensity monitoring. *International Journal of Applied Earth Observations and Geoinformation, 94*, Article Number: 102222. https://doi.org/10.1016/j.jag.2020.102222

19. Mousavi-Baygi, M., Ashraf, B., & Miyanabady, A. (2010). The Investigation of Tehran's heat island by using the surface ozone and temperature data. *International Journal of Applied Environmental Sciences,5*(2),189-200. https://www.researchgate.net/publication/268327877_The_Investigation_of_Tehran%27s_Heat_Island_by_using_the_Surface_Ozone_and_Temperature_Data

20. Oke, T.R. (1979). City size and the urban heat island. *Atmospheric Environment Pergamon Press, 7*, 769-779. https://www.patarnott.com/pdf/Oke1979CitySizeAndHeatIsland.pdf

21. Oke, T.R. (1982). The energetic basis of urban heat island. *Journal of the Royal Meteorological Society , 108*, 1-24. https://www.patarnott.com/pdf/Oake1982_UHI.pdf

22. Rajeshwari, A., & Mani, N.D. (2014). Estimation of land surface temperature of Dindigul district using Landsat 8 data. *International Journal of Research in Engineering and Technology, 3*,122-126. https://ijret.org/volumes/2014v03/i05/IJRET20140305025.pdf

23. Rizwan, A.M., Dennis, L.Y., & Liu, C. (2008). A review on the generation, determination and mitigation of urban heat island. *Journal of Environmental Sciences, 20*(1), 120-128. https://doi.org/10.1016/S1001-0742(08)60019-4

24. Sadeghinia, A., Alijani, B., Ziaeian, P., & Khaledi, S. (2013). Application of spatial autocorrelation techniques in the analysis of the thermal island of Tehran. *Applied Research in Geographical Sciences , 13*(30), 67-90. https://www.sid.ir/en/Journal/ViewPaper.aspx?ID=354812 (In Persian).

25. Sekertekin, A., & Zadbagher, E. (2021). Simulation of future land surface temperature distribution and evaluating surface urban heat island based on impervious surface area. *Ecological Indicators, 122* ,Article Number: 107230. https://doi.org/10.1016/j.ecolind.2020.107230

26. Tepanosyan, G., Muradyan, V., Hovsepyan, A., Pinigin, G., Medvedev, A., & Asmaryan, Sh. (2021). Studying spatial-temporal changes and relationship of land cover and surface Urban Heat Island derived through remote sensing in Yerevan. *Armenia Building and Environment, 187*, Article Number: 107390. https://doi.org/10.1016/j.buildenv.2020.107390

27. Van de Griend, A., & Owe, M. (1993). On the relationship between thermal emissivity and the normalized difference vegetation index for natural surfaces. *International Journal of Remote Sensing, 14*(6), 1119-1131. https://doi.org/10.1080/01431169308904400

28. Vasenev, V., Varentsova, M., Konstantinov, P., Romzaykina, O., Kanareykina, I., Dvornikov, V., & Manukyana, Y. (2021). Projecting urban heat island effect on the spatial-temporal variation of microbial respiration in urban soils of Moscow megalopolis. *Science of the Total Environment,786*(10), Article number: (147457). https://doi.org/10.1016/j.scitotenv.2021.147457

29. Wang, W., Liu, K., Tang, R., & Wang, Sh. (2019). Remote sensing image-based analysis of the urban heat island effect in Shenzhen. *China Physics and Chemistry of the Earth*, *110*, 168-175. https://doi.org/10.1016/j.pce.2019.01.002

30. Wang, Y., Yi, G., Zhou, X., Zhang, T., Bie, X., Li, J., & Ji, B. (2021). Spatial distribution and influencing factors on urban land surface temperature of twelve megacities in China from 2000 to 2017. *Ecological Indicators*, *125*, Article Number: 107533. https://doi.org/10.1016/j.ecolind.2021.107533

31. Wei, B., Bao, Y., Yu, Sh., Yin, Sh., & Zhang, Y. (2021). Analysis of land surface temperature variation based on MODIS data a case study of the agricultural pastural ecotone of northern China. *International*

Journal of Applied Earth Observations and Geoinformation, *100*, Aarticle number: 102342. https://doi.org/10.1016/j.jag.2021.102342

32. Weng, Q. (2009). Thermal infrared remote sensing for urban climate and environmental studies: Methods, applications, and trends. *ISPRS Journal of Photogrammetry and Remote Sensing* , *64*(4), 335-344. https://doi.org/10.1016/j.isprsjprs.2009.03.007

33. Ye, X., Ren, H., Liang, Y., Zhu, J., Guo, J., Nie, J., Zeng, H., Zhao, Y., & Qian, Y. (2021). Cross-calibration of Chinese Gaofen-5 thermal infrared images and its improvement on land surface temperature retrieval. *International Journal of Applied Earth Observations and Geoinformation*, 101, Article number: 102357. https://doi.org/10.1016/j.jag.2021.102357